RSC Advances

PAPER

View Article Online
View Journal | View Issue

Cite this: *RSC Adv.*, 2017, **7**, 25528

A turn-on green channel Zn^{2+} sensor and the resulting zinc(II) complex as a red channel HPO_4^{2-} ion sensor: a new approach†

Somenath Lohar,[a] Siddhartha Pal,[a] Manjira Mukherjee,[a] Abhishek Maji,[a] Nicola Demitri[b] and Pabitra Chattopadhyay *[a]

A newly synthesized and spectroscopically characterized non-fluorescent organic moiety (**L′H**) selectively sensed Zn^{2+} ions based on a chelation-enhanced fluorescence (CHEF) process at the λ_{em} of 520 nm through the formation of a new dinuclear zinc(II) complex (**1**). Upon the addition of Zn^{2+} ions to the solution of **L′H** in dimethyl sulphoxide at 25 °C, a systematic enhancement of fluorescence was observed, which was not affected by the presence of competitive ions. The reaction of **L′H** with Zn^{2+} ions led to the formation of a dinuclear zinc(II) complex, featuring a new *in situ* formed macrocyclic ligand (**L**), which was isolated in pure form and then characterized. The formulation of **1** was established by spectroscopic tools along with a detailed structural analysis carried out using single crystal X-ray crystallography. In addition, the complex **1** also behaved as a red-shifted, HPO_4^{2-} ion-selective chemosensor at the λ_{em} of 595 nm based on a displacement approach in dimethyl sulphoxide. Interestingly, **1** showed remarkable sensitivity towards HPO_4^{2-} ions *via* fluorescence modulation of the dinuclear zinc(II) complex (**1**) compared with the other anions examined herein.

Received 21st February 2017
Accepted 14th April 2017

DOI: 10.1039/c7ra02175e

rsc.li/rsc-advances

Introduction

Designing highly sensitive and specific sensors for ionic species is of great interest because of biological and environmental applications of these sensors.[1–3] These ions are vital because of their sustainable role in the biological processes of living beings. Zinc ion (Zn^{2+}) is the second most abundant metal ion in the human body, and the cellular biochemistry of Zn^{2+} is diverse and far ranging.[4] Moreover, misregulation of Zn^{2+} is also implicated in human health disorders. It is believed that lack of zinc ions can result in an increased risk of several disorders, such as stunted growth, mental retardation, and digestive dysfunction, because majority of biological zinc ions are tightly sequestered by proteins.[5] Additionally, the presence of excess free zinc in certain cells may be related to severe neurological disorders such as Alzheimer's and Parkinson's disease.[6a,b] Therefore, it is necessary to obtain insight into the vital roles of Zn^{2+} ions in biological processes, resulting in great demand for the design and development of efficient systems that can selectively and sensitively detect Zn^{2+} in living systems. Several analytical methods including UV-vis-spectroscopy,[6c] potentiometry,[6d] and flame atomic absorption spectrometry[6e] have played a vital role in the detection of Zn^{2+}. A variety of fluorescent sensors for Zn^{2+} have been reported based on various fluorophores,[7–9] and continuous efforts have been dedicated to improve the effectiveness of Zn^{2+} sensors.

The development of selective receptors for phosphate anions and derivatives, such as HPO_4^{2-}, $H_2PO_4^-$, pyrophosphate (PPi, $P_2O_7^{4-}$), adenosine triphosphate (ATP), adenosine diphosphate (ADP), CTP_3, IP_3, and phosphoproteins,[10] has been of particular interest because of the vital roles that these chemical species play in a range of life processes. These processes involve essential events such as energy storage, signal transduction, and gene construction. Especially, PPi is a biologically important target because it is the product of ATP hydrolysis under cellular conditions.[11] Similarly, ATP is also a very important sensing target because it is known as a universal energy source and is also involved in many enzymatic reactions inside living organisms.[11] Therefore, the development of a quick and sensitive method for phosphate anion detection is of great importance. Recently, metal-based receptors, particularly Zn(II) complexes, for fluorescence sensing of $H_2PO_4^-$ ions, pyrophosphate, and phosphate[12] have been reported; however, a dinuclear zinc(II) complex as a HPO_4^{2-} ion sensor has not been reported to date.

[a]*Department of Chemistry, The University of Burdwan, Golapbag, Burdwan 713104, India. E-mail: pabitracc@yahoo.com; Fax: +91 342 2530452; Tel: +91 342 2558554 extn 424*

[b]*Elettra – Sincrotrone Trieste, S.S. 14 Km 163.5 in Area Science Park, 34149 Basovizza, Trieste, Italy*

† Electronic supplementary information (ESI) available: Materials and physical methods, tables, figures, characterization data, and some spectra. CCDC 1528839. CCDC no. for dinuclear zinc(II) complex (**1**). For ESI and crystallographic data in CIF or other electronic format see DOI: 10.1039/c7ra02175e

Due to high sensitivity, rapid response rate, and the relatively low-cost of fluorescence systems, significant attention has also been paid to developing fluorescent chemosensors capable of recognizing and sensing both cations and anions.[13] In most cases, enhancement or the turn-on of fluorescence towards one species and the resulting complex acting as a quencher or turn-off for another species at the same emission wavelength, or *vice versa*, have been reported.[14] In some cases, a change in solvent has played a key role in evaluating a sensor for two ions at different emission wavelengths.[15] Herein, an organic moiety selectively sensed Zn^{2+} ions with green fluorescence (λ_{em}: 520 nm) at a concentration as low as 27.80 nM, and the resulting zinc(II) complex (**1**) effectively detected HPO_4^{2-} ions with red fluorescence (λ_{em}: 595 nm) in the same solvent, DMSO, on excitation at the same wavelength (λ_{ex}: 440 nm). To the best of our knowledge, to date, this type of an organic moiety and the resulting zinc(II) complex have not been explored as sensors based on the enhancement of fluorescence at different emission wavelengths through a significant amount of a red-shift of *ca.* 75 nm.

Herein, we present a new fluorescent and colorimetric chemosensor, 4-methyl-2,6-bis-[(5-phenyl-1*H*-pyrazol-3-ylimino)-methyl]-phenol (**L′H**), for the selective sensing of Zn^{2+} ions and the dinuclear zinc(II) complex of a new *in situ* formed macrocyclic type ligand (**L**); this complex resulted from the reaction of **L′H** with Zn^{2+} ions, which formulated $\mathbf{Zn_2L}$ (**1**) that is selective for HPO_4^{2-} anions in a DMSO solution. The **L′H** selectively senses Zn^{2+} ions based on a chelation-enhanced fluorescence (CHEF) process, whereas the structurally characterised zinc(II) complex (**1**) performs as a red-shifted, HPO_4^{2-} ion selective chemosensor based on a displacement approach in dimethyl sulphoxide. The complex **1** showed selective UV-vis and fluorescence responses for the biologically relevant HPO_4^{2-} anion in DMSO with a low detection limit even in the presence of several other anions.

Experimental

Synthesis of 4-methyl-2,6-bis-[(5-phenyl-1*H*-pyrazol-3-ylimino)-methyl]-phenol (L′H)

A solution of 3-amino-5-phenylpyrazole (1.59 g, 10.0 mmol) in absolute methanol (10 mL) was added dropwise to a stirred solution of 2,6-diformyl-4-methyl-phenol (0.82 g, 5.0 mmol) in the same solvent (20 mL). The resulting solution was gently refluxed under magnetic stirring for *ca.* 6 h. The yellow powder precipitate that formed was filtered off, washed several times with absolute methanol, dried under vacuum, and characterized as compound **L′H**.

L′H. $C_{27}H_{22}N_6O$. Calcd C, 72.63; H, 4.97; N, 18.82; O, 3.58; anal. found: C 72.34, H 4.39, N 18.95. Mp 292 ± 2 °C. ESI-MS: [**L** + H^+], *m*/*z*, 447.1939 (obs. with 100% abundance) [(calcd: *m*/*z*, 447.198; where **L′H** = molecular weight of organic moiety (**L′H**))]; ^{1}H NMR (DMSO-d_6, 400 MHz, δ ppm): 2.32 (s, 3H), 6.72–6.77 (s, 2H), 7.23–7.43 (m, 8H), 7.73–7.96 (m, 4H), 9.18 (s, 2H), 10.40 (s, 1H) and 13.42 (broad, 2H). ^{13}C NMR (DMSO-d_6): 162.87, 159.86, 150.05, 144.39, 140.03, 137.83, 129.85, 129.48, 125.98, 124.18, 121.27, 94.91 and 20.87. IR (KBr, cm^{-1}): ν_{OH}: 3411.46, $\nu_{CH=N}$: 1561.08, ν_{NH}: 1455.53, 1426.74. Yield, 97%.

Synthesis of dinuclear zinc(II) complex (1)

To the dimethylformamide (DMF) solution of **L′H** (446.0 mg, 1.0 mmol), a water solution of zinc nitrate hexahydrate (149.00 mg, 0.50 mmol) was very slowly added under vigorous stirring. Then, the reaction mixture was stirred at ambient temperature for another 6.0 h. The resulting solution was kept aside for slow evaporation at room temperature. After a few days, a red-coloured crystalline solid was obtained. Single crystals suitable for X-ray analysis were obtained from the solution of the crude product in DMF–H_2O on slow evaporation.

$[Zn_2L]\cdot 3H_2O$. $C_{90}H_{72}N_{18}O_7Zn_2$. Anal. found: C, 66.15; H, 4.53; N, 15.76; calc.: C, 66.30; H, 4.33; N, 15.46. IR (cm^{-1}): ν_{NH} = 3427.45; $\nu_{CH=N}$ = 1577.07. ^{1}H NMR (500 MHz, DMSO-d_6): 10.18 (s, 1H); 8.85 (d, 1H; j = 50.5 Hz); 8.70 (s, 3H); 7.48 (m, 9H); 7.40 (m, 11H); 7.20 (m, 24H); 6.88 (b, 3H); 6.55 (s, 2H); 5.76 (s, 1H); 5.56 (b, 3H); 2.27 (s, 8H). ESI-MS (in methanol): $[M + 2H]^{2+}$, *m*/*z*, 798.12 (100%) [(calcd: *m*/*z*, 798.21; where M = molecular weight of $C_{90}H_{66}N_{18}O_4Zn_2$)] yield, 63%.

X-ray crystallography

Data collection of compound **1** was performed at the X-ray diffraction beamline (XRD1) of the Elettra Sincrotrone Trieste (Italy), with a Pilatus 2M image plate detector. The complete dataset was obtained at 100 K (nitrogen stream supplied by an Oxford Cryostream 700) with a monochromatic wavelength of 0.700 Å through the rotating crystal method. The crystals were dipped in *N*-paratone and mounted on the goniometer head with a nylon loop. The diffraction data were indexed, integrated, and scaled using XDS.[16] The structure was solved by direct methods using SIR2014 [17] and subsequent Fourier analysis, and refinement with the full-matrix least-squares method based on F^2 was performed with SHELXL.[18] Anisotropic thermal motion was allowed for all the non-H atoms. Hydrogen atoms were placed at the calculated positions, except those of the coordinated water molecules. The void in the unit cell (18.5%) was taken into account using the Squeeze program (Platon) since the solvent molecules could not be suitably modelled and refined. Graphics were drawn using the Cameron program.[19] The dinuclear zinc(II) complex (**1**) crystallized in the monoclinic space group *Pc*. Crystal data and details are tabulated in Table S1,† and some selected bond distances and angles are listed in Table S2.†

General method of UV-vis and fluorescence titration

For UV-vis and fluorescence titrations, stock solutions of **L′H** and dinuclear zinc(II) complex (**1**) were prepared in DMSO and a stock solution of Zn^{2+} and HPO_4^{2-} was prepared in HPLC water at 25 °C. Fluorescence measurements were carried out using a 2.5 nm *x* 2.5 nm slit width. To the 100 μL (5 μM) stock solution of **L′H**, 0–300 μL (0–15 μM) Zn^{2+} solution was gradually added, and the total volume was adjusted to 2.0 mL by adding the required amount of DMSO to obtain the absorbance and fluorescence spectra. Similarly, a HPO_4^{2-} solution (0–150 μL)

(0–75 μM) was gradually added to the 50 μL (25 μM) stock solution of the dinuclear zinc(II) complex (**1**), and the total volume was adjusted to 2 mL by the addition of DMSO. All the spectral data were acquired after 10 minutes of mixing to obtain the optimized spectra.

Result and discussion

Synthesis and structural characterisation

The organic moiety 4-methyl-2,6-bis-[(5-phenyl-1*H*-pyrazol-3-ylimino)-methyl]-phenol (**L′H**) was synthesized by condensing a methanolic solution of 3-amino-5-phenylpyrazole with 2,6-diformyl-4-methyl-phenol in a 2 : 1 ratio (Scheme 1). The formulation of **L′H**, as shown in Scheme 1, was established by physicochemical and spectroscopic tools. The peaks obtained in the ^{1}H NMR spectrum of **L′H** were assigned, and these were in agreement with the structural formula of this ligand in solution (Fig. S1†). The ESI mass spectrum of the compound in methanol showed a peak at *m*/*z* 447.1939 with 100% abundance assignable to [**L′H** + H$^+$] (calculated value at *m*/*z* 447.198), where **L′H** = molecular weight of the organic moiety (Fig. S2†). The IR spectrum of **L′H** showed the characteristic stretching of O–H, N–H, and C=N bonds (Fig. S3†), and the characteristic peaks were observed in the ^{13}C NMR spectrum (Fig. S4†).

The dinuclear zinc(II) complex (**1**) was isolated in the solid state from the reaction mixture of **L′H** with zinc nitrate hexahydrate in a 2 : 1 molar ratio in a DMF/water medium at room temperature under stirring condition. Upon reaction of **L′H** with Zn^{2+} ions, a new *in situ* macrocyclic type ligand (**L**) was formed and red-colored single crystals of $\mathbf{Zn_2L}\cdot H_2O$ were obtained on slow evaporation. The well-resolved ESI mass spectrum (Fig. S5†), IR spectrum (Fig. S6†), and ^{1}H NMR spectrum (Fig. S7†) of the dinuclear zinc(II) complex (**1**) support the formulation and the structure established by single crystal X-ray crystallographic analysis. Of the two zinc ions, Zn1 exhibited an octahedral coordination sphere realized through two phenolato oxygen and two imine nitrogen atoms, completing its coordination geometry with two aqua ligands. Zn2 presented a highly distorted octahedral environment by being chelated by two oxygen and two imine nitrogen donors (Fig. 1).

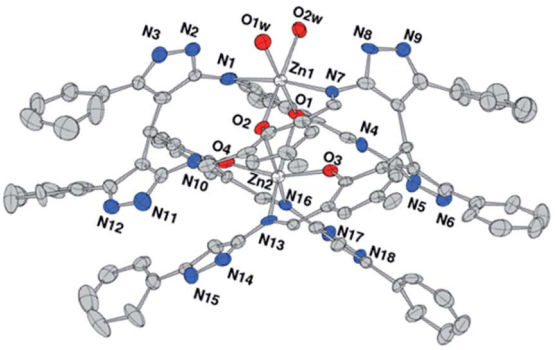

Fig. 1 ORTEP drawing (ellipsoids at 30% probability) of the dinuclear complex $\mathbf{Zn_2L}$ (H atoms omitted for clarity).

UV-vis spectroscopy studies of L′H

The UV-vis absorption spectrum of **L′H** obtained in DMSO solution exhibited intense absorption bands at energy levels below 400 nm, corresponding to $\pi \rightarrow \pi^*$ (275 nm, $\varepsilon = 2.1 \times 10^5$ L mol^{-1} cm^{-1}; 315 nm, $\varepsilon = 1.61 \times 10^5$ L mol^{-1} cm^{-1}) and n $\rightarrow$ π^* (380 nm, $\varepsilon = 2.4 \times 10^4$ L mol^{-1} cm^{-1}) transitions. To evaluate the binding affinity of **L′H** towards Zn^{2+} ions, the UV-vis spectral changes upon the addition of Zn^{2+} ions to the solution of **L′H** in DMSO were investigated. The incremental addition of Zn^{2+} ions led to a gradual decrease in the absorbance along with the appearance of a lower-energy metal-to-ligand charge-transfer (MLCT) band at around 440 nm. The presence of an isosbestic point at 410 nm indicated the existence of an equilibrium between two species: **L′H** and the resulting dinuclear zinc(II) complex (**1**) (Fig. 2).

To verify the potential of the probe **L′H** in the intracellular atmosphere, another inspection of the probe was carried out to check the interferences of other competitive ions. Metal ion selectivity assays were performed without changing other experimental conditions. On the addition of an excess of 10

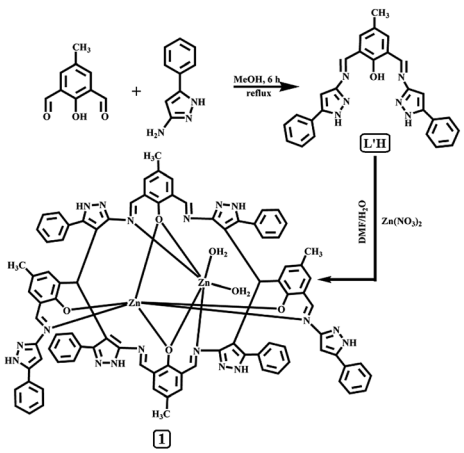

Scheme 1 Synthetic strategy of L′H and $\mathbf{Zn_2L}$-complex (**1**).

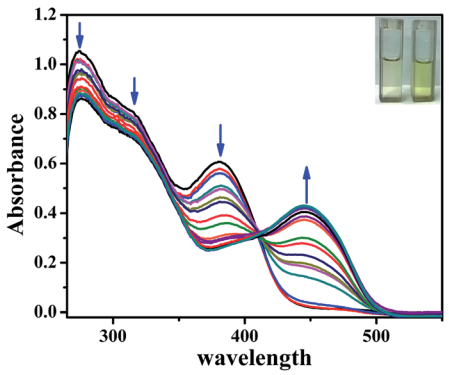

Fig. 2 UV-vis titration spectra of L′H (5 μM) with Zn^{2+} ions (0–15 μM) in DMSO solution at 25 °C with naked eye visual color change of L′H only and Zn(II) complex (**1**) [in inset].

equivalents of relevant metal ions (*i.e.*, Cr^{3+}, Mn^{2+}, Fe^{3+}, Co^{2+}, Ni^{2+}, Cu^{2+}, Cd^{2+}, Hg^{2+}, Na^{+}, K^{+}, Ca^{2+}, Mg^{2+}, Al^{3+}, and Pb^{2+}), no significant change was observed in the UV-vis spectral pattern.

Fluorescence studies of L′H

The organic probe **L′H** exhibited a very feeble emission intensity at 520 nm (λ_{ex}: 440 nm). Upon incremental addition of Zn^{2+} ions (0–15 μM), the fluorescence intensity steadily and significantly increased by about ~11-fold at 520 nm (Fig. 3). This spectral characteristic for the addition of Zn^{2+} ions was supported by the shift from colourless to fluorescent green. To check the saturation time of the resulting emission, the time-dependent profile for the fluorescent detection of Zn^{2+} ions (Fig. S8†) was also obtained under the same conditions, and it was determined to be 15 min. From the fluorimetric titration curve, a plot of the fluorescence intensity *vs.* concentration of Zn^{2+} ions is depicted in Fig. S9.†

The emission intensity increased due to addition of Zn^{2+} ions (0–15 μM) to the solution of **L′H** (5 μM) with an enhancement of the fluorescence quantum yield[20] by *ca.* three times (Φ = 0.157) in DMSO, which was calculated by integrating the area under the fluorescence curves using the following equation:

$$\Phi_{sample} = \Phi_{ref} \times \frac{OD_{ref} \times A_{sample} \times \eta_{sample}^{2}}{OD_{sample} \times A_{ref} \times \eta_{ref}^{2}}$$

where A is the area under the fluorescence spectral curve, OD is the optical density of the compound at the excitation wavelength 440 nm, and η is the refractive index of the solvent used. The standard used for the measurement of fluorescence quantum yield was fluorescein (Φ = 0.79 in a 0.1 M NaOH solution).

Selectivity

The selectivity study of the organic moiety **L′H** towards various cations was carried out using transition metal ions (Cr^{3+}, Mn^{2+}, Fe^{3+}, Co^{2+}, Ni^{2+}, Cu^{2+}, Zn^{2+}, Cd^{2+}, and Hg^{2+}), alkali and alkaline earth metal ions (Na^{+}, K^{+}, Ca^{2+}, and Mg^{2+}), and some other metal ions (Al^{3+} and Pb^{2+}) (Fig. S10†), having a concentration 50 times that of the ligand. The organic moiety (**L′H**) had a remarkable specificity and selectivity towards Zn^{2+} ions over the other metal ions examined herein. Interestingly, the introduction of other metal ions caused the emission intensity to be either weakened or unchanged. In the presence of a 10 equivalent excess of various tested ions together with **L′H** and Zn^{2+} ions, no adverse effect on the intensity was observed (Fig. S11†).

Job's plot from fluorescence experiments

A series of solutions containing **L′H** and Zn^{2+} ions were prepared such that the total concentration of the sample solution remained constant (20 μM) in all the sets. The mole fractions of Zn^{2+} ions were varied from 0.1 to 0.8. The emission intensity (for **L′H**) at 520 nm was plotted against the mole fraction of [Zn^{2+}] ions. From a Job's plot analysis (Fig. S12†), it was revealed that the maximum emission was at 2 : 1 ratio. These data indicate that the complex species in solution should form a 2 : 1 complex with Zn^{2+} ions, in accordance with the single crystal observations.

Effect of pH

A pH study was performed for the probe **L′H** in the absence and presence of Zn^{2+} ions over the pH range of 4.0–11.0 (Fig. S13†).

Detection limit calculation

The detection limit was calculated from the calibration curve based on the fluorescence enhancement at 520 nm (Fig. 4) focusing on the lower concentration region of Zn^{2+} ions. From the slope of the curve (S) and the standard deviation of seven replicate measurements of the zero level (σ_{zero}), the detection limit was estimated using the equation $3\sigma/S$.[21] The data obtained from this graph indicated that this probe can effectively detect Zn^{2+} ion at very low concentrations up to 27.80 nM.

Spectroscopic studies of dinuclear zinc(II) complex (1)

Absorption study. The UV-vis absorption spectrum of **1**, obtained in the DMSO solution, exhibited intense absorption-bands at the energy levels at 440 nm due to metal-to-ligand charge-transfer (MLCT) transitions. To find the binding affinity of **1** towards HPO_4^{2-}, the spectral changes by the

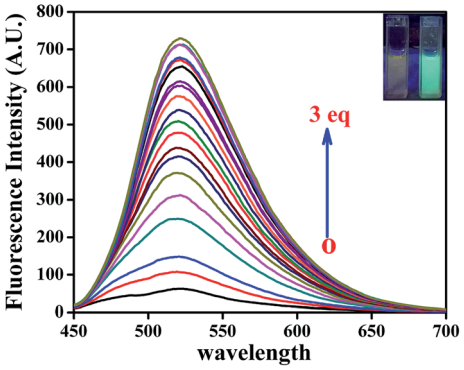

Fig. 3 Fluorescence titration of L′H (5 μM) with the incremental addition of Zn^{2+} ions (0–15 μM) DMSO solution with naked eye fluorescence color change L′H only and zinc(II) complex (**1**) [in inset].

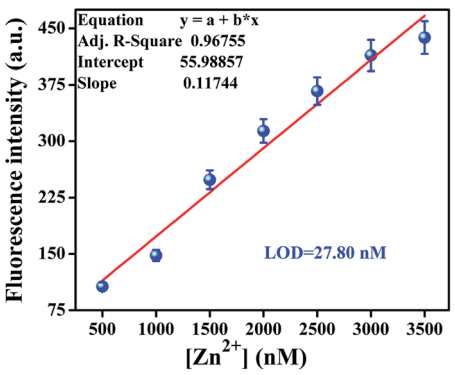

Fig. 4 Calibration curve in the nanomolar range to calculate the LOD of Zn^{2+} ions by L′H in DMSO solution.

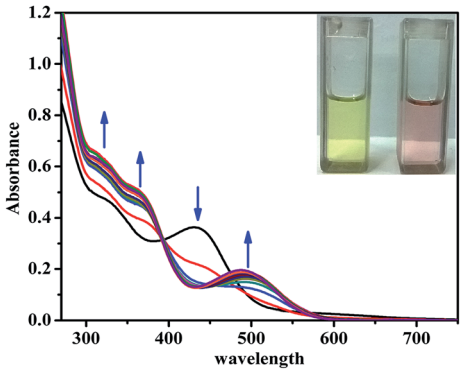

Fig. 5 UV-vis titration spectra of **1** (25 μM) with HPO_4^{2-} ions (0–75 μM) in DMSO solution at 25 °C. Naked eye visual color change of **1** only and **1** in presence of HPO_4^{2-} ions [inset].

addition of HPO_4^{2-} ions to the DMSO solution of **1** were investigated. The incremental addition of HPO_4^{2-} ions to **1** led to a decrease in the intensity of the band at 432 nm with an appearance of new bands at around 315, 365, and 495 nm (Fig. 5).

Emission study. The displacement of Zn^{2+} ions from the complex (**1**) by HPO_4^{2-} ions was studied from the emission spectral change of the titration curve, as shown in Fig. 6. For the emission study, DMSO solution was continuously titrated with an increasing concentration of HPO_4^{2-} ions. The spectra show the generation of a red-shifted emission band with a maximum at ~595 nm. The continuous increase in the HPO_4^{2-} ions concentration (Fig. S14†) led to a concomitant enhancement of the emission band with a maximum at ~595 nm. The resultant solution was kept undisturbed for 15 min, and then, the emission spectrum was obtained considering the time-dependent profile for the fluorescent detection of HPO_4^{2-} ions, as shown in Fig. S15.† The emission intensity increased due to addition of HPO_4^{2-} ions (0–75 μM) to the solution of **1** (25 μM), with the enhancement of fluorescence quantum yield by *ca.* two times (Φ = 0.3421) in DMSO, which was calculated by integrating the area under the fluorescence curves.

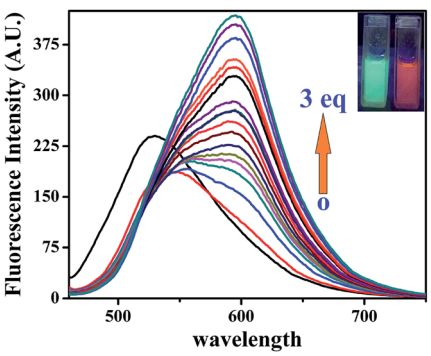

Fig. 6 Fluorescence titration of **1** (25 μM) with the incremental addition of HPO_4^{2-} ions (0, 2.5, 5, 10, 15, 20, 25, 30, 35, 40, 45, 50, 55, 60, 65, 70, and 75 μM) in DMSO solution (λ_{ex} = 440 nm). Naked eye fluorescence color change **1** only and **1** in presence of HPO_4^{2-} ions [inset].

To examine the efficacy of the resulting dinuclear zinc(II) complex (**1**), herein, the rupture of the dinuclear zinc(II) complex (**1**) to restore **L′H** and the subsequent change in the spectral properties of the dinuclear zinc(II) complex (**1**) in DMSO were studied towards different anions (SCN^-, PO_4^{3-}, MO_4^{2-}, CN^-, F^-, Cl^-, Br^-, I^-, $HAsO_4^{2-}$, AcO^-, HPO_4^{2-}, $H_2AsO_4^-$, SO_4^{2-}, $H_2PO_4^-$, HSO_4^-, NO_3^-, CO_3^{2-}, HCO_3^-, ClO_4^-, and $P_2O_7^{4-}$ (1 equiv., as sodium/potassium salts)). The binding studies exhibited a fast, sensitive, and distinct response towards HPO_4^{2-} ions in comparison to the other anions (Fig. S16†). In the fluorescence spectrum, upon addition of HPO_4^{2-} ions, the emission band at 520 nm was quenched, and a new red-shifted band at 595 nm appeared. This result indicated the weakening of the existing dinuclear zinc(II) complex (**1**) bond due to the interaction of HPO_4^{2-} ions with Zn^{2+} ions to form $Zn(HPO_4)$ species, insoluble in this medium. Almost no interference was observed for the detection of HPO_4^{2-} anions even in the presence of other anions, having 50 times higher concentration (Fig. S16†).

The detection limit was calculated from the calibration curve based on the fluorescence enhancement at 595 nm (Fig. S17†) focusing on the lower concentration region of HPO_4^{2-} anions. From the slope of the curve (S) and the standard deviation of seven replicate measurements of the zero level (σ_{zero}), the detection limit was estimated using the equation $3\sigma/S$.[21] The data obtained from this graph indicates that this probe can effectively detect HPO_4^{2-} anions at very low concentrations up to 3.12×10^{-7} M.

The emission spectra of **L′H**, **L′H** + Zn^{2+} ion (**1**), and **1** + HPO_4^{2-} ions were also obtained with the increasing solvent polarity, as shown in Fig. S18.† From this study, it was revealed that the polarity of the solvent had almost no effect on the emission wavelength (λ_{em}) but had an effect on the emission intensity, which was highest in DMSO in both cases.

The turn on green fluorescence (λ_{em} = 520 nm) was due to the formation of a new dinuclear zinc(II) complex (**1**), which was based on chelation-enhanced fluorescence (CHEF) process, and

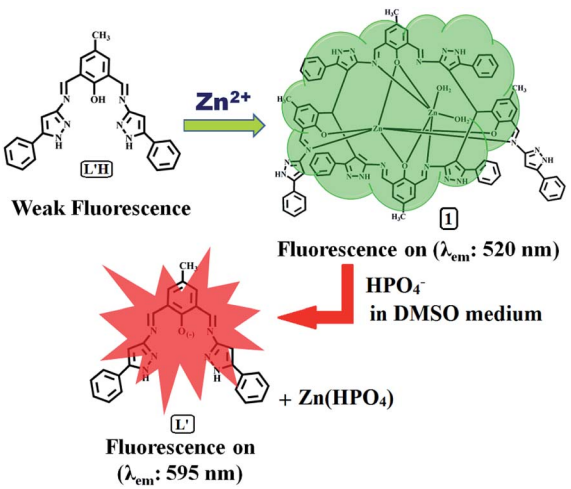

Scheme 2 Probable mechanism for Zn^{2+} sensing by L′H and HPO_4^{2-} ions sensing by the Zn(II) complex (**1**).

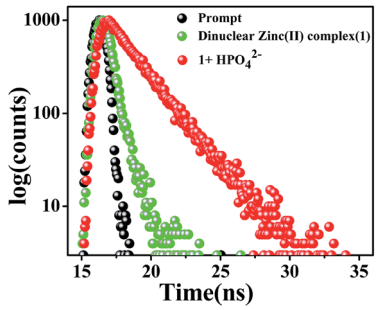

Fig. 7 Time-resolved fluorescence decay of dinuclear zinc(II) complex (**1**) and **1** in the presence of HPO_4^{2-} ions (at λ_{em} = 595 nm) in DMSO using a nano-LED at 470 nm as the light source.

the fluorescence arose due to the formation of a dinuclear zinc(II) complex of a newly *in situ* formed macrocyclic ligand (**L**) during the reaction of **L′H** with Zn^{2+} ions.

The displacement mechanistic pathway in the complex (**1**) by hydrogen phosphate anion was established by UV-vis and fluorescence spectra (Fig. S19†), ESI mass spectra (Fig. S20†), and ^{1}H NMR spectra (Fig. S21†). We obtained a new absorption peak at *ca.* 495 nm due to the addition of HPO_4^{2-} anions to the zinc(II) complex (**1**); moreover, a similar type of peak was obtained at *ca.* 495 nm in the case of **L′H** in the presence of a base, a signature of the anionic species **L′** (*viz.* Fig. S13†) formed with a high fluorescence quantum yield (Φ = 0.300). The findings from these studies indicate that the appearance of the red fluorescence (λ_{em} = 595 nm) of **1** upon the gradual addition of HPO_4^{2-} anions was due to the formation of a deprotonated form of **L′H**. On the basis of these spectroscopic observations, a plausible sensing pathway is shown in Scheme 2.

TCSPC experiment

To strengthen the proposed mechanism, the fluorescence average life time measurement of **1** was performed, and it was found to be 0.56 ns at λ_{em} = 595 nm. The average lifetime of the formed species, due to the addition of HPO_4^{2-} ions to the solution of **1**, increased to 2.25 ns at λ_{em} = 595 nm (*viz.* **1** : HPO_4^{2-}; 1 : 1 in Fig. 7). According to the equations:[22] $\tau^{-1} = k_r + k_{nr}$ and $k_r = \Phi_f/\tau$, the radiative rate constant k_r and total nonradiative rate constant k_{nr} of dinuclear zinc(II) complex (**1**) in the absence and presence of HPO_4^{2-} ions are listed in Table S3.† The data suggests that the k_r/k_{nr} ratio was reasonably enhanced due to the reasonable decrease of k_{nr} in support of the increased in fluorescence in the presence of HPO_4^{2-} ions at λ_{em} = 595 nm.

Conclusions

A new non-fluorescent Schiff base-type organic probe (**L′H**) was synthesized and spectroscopically characterised. **L′H** selectively sensed Zn^{2+} ions based on a chelation-enhanced fluorescence (CHEF) process at a λ_{em} of 520 nm (green fluorescence) through the formation of a new dinuclear zinc(II) complex (**1**) with almost no interference of competitive ions. A red-colored solid dinuclear zinc(II) complex of a new *in situ* formed macrocyclic-type ligand (**L**), formulated as $\mathbf{Zn_2L}$, (**1**) was isolated from the reaction mixture of **L′H** with Zn^{2+} ions and was characterized by spectroscopic tools along with detailed structural analyses using single crystal X-ray crystallography. Interestingly, complex (**1**) also selectively sensed HPO_4^{2-} anions with a red fluorescence (λ_{em}: 595 nm) in the same solvent, DMSO, on excitation at the same wavelength (λ_{ex}: 440 nm).

Acknowledgements

The financial assistance received from Department of Science and Technology, Govt. of West Bengal (DST, GoWB, *vide* project no. 698 (Sanc.)/ST/P/S & T/15-G/2015) is gratefully acknowledged. S. Lohar is thankful to UGC, New Delhi, India for the fellowship.

Notes and references

1 (*a*) D. Li, L. Liu and W. H. Li, *ACS Chem. Biol.*, 2015, **10**, 1054; (*b*) Y. Ding, Y. Tang, W. Zhu and Y. Xie, *Chem. Soc. Rev.*, 2015, **44**, 1101; (*c*) Z. Guo, G. H. Kim, I. Shin and J. Yoon, *Biomaterial*, 2012, **33**, 7818; (*d*) K. Tayade, S. K. Sahoo, B. Bondhopadhyay, V. K. Bhardwaj, N. Singh, A. Basu, R. Bendre and A. Kuwar, *Biosens. Bioelectron.*, 2014, **61**, 429; (*e*) H. Tapiero and K. D. Tew, *Biomed. Pharmacother.*, 2003, **61**, 399.

2 (*a*) J. Yoon, S. K. Kim, N. J. Singh and K. S. Kim, *Chem. Soc. Rev.*, 2006, **35**, 355; (*b*) R. Martínez-Manez and F. Sancanon, *Chem. Rev.*, 2003, **103**, 4419; (*c*) J. F. Callan, A. P. de Silva and D. C. Magri, *Tetrahedron*, 2005, **61**, 8551.

3 (*a*) L. Fabbrizzi, M. Licchelli, G. Rabaioli and A. Taglietti, *Coord. Chem. Rev.*, 2000, **205**, 85; (*b*) P. A. Gale, *Acc. Chem. Res.*, 2006, **39**, 465.

4 (*a*) A. I. Bush, W. H. Pettingell, G. Multhaup, M. Paradis, J. P. Vonsattel, J. F. Gusella, K. Beyreuther, C. L. Masters and R. E. Tanzi, *Science*, 1994, **265**, 1464; (*b*) C. J. Frederickson, J. Y. Koh and A. I. Bush, *Nat. Rev. Neurosci.*, 2005, **6**, 449; (*c*) D. D. Mott, M. Benveniste and R. J. Dingledine, *J. Neurosci.*, 2008, **28**, 1659; (*d*) J. M. Berg and Y. Shi, *Science*, 1996, **271**, 1081.

5 A. Krężel and W. Maret, *J. Biol. Inorg Chem.*, 2006, **11**, 1049.

6 (*a*) A. I. Bush, *Trends Neurosci.*, 2003, **26**, 207; (*b*) D. Noy, I. Solomonov, O. Sinkevich, T. Arad, K. Kjaer and I. Sagi, *J. Am. Chem. Soc.*, 2008, **130**, 1376; (*c*) C. V. Banks and R. E. Bisque, *Anal. Chem.*, 1957, **29**, 522; (*d*) A. R. Fakhari, M. Shamsipur and K. H. Ghanbari, *Anal. Chim. Acta*, 2002, **460**, 177; (*e*) Q. Li, X. H. Zhao, Q. Z. Lv and G. G. Liu, *Sep. Purif. Technol.*, 2007, **55**, 76.

7 (*a*) K. K. Upadhyay, A. Kumar, J. Zhao and R. K. Mishra, *Talanta*, 2010, **81**, 714; (*b*) J. F. Zhang, S. Kim, J. H. Han, S. J. Lee and J. S. Kim, *Org. Lett.*, 2011, **13**, 5294; (*c*) Y. Xu, J. Meng, L. X. Meng, Y. Dong, Y. X. Cheng and C. J. Zhu, *Chem.–Eur. J.*, 2010, **16**, 12898; (*d*) Q. H. You, P. S. Chan, W. H. Chan, N. K. Mak and R. N. S. Wong, *RSC Adv.*, 2012, **2**, 11078; (*e*) H. Y. Lin, P. Y. Cheng, C. F. Wan and A. T. Wu, *Analyst*, 2012, **137**, 4415.

8 (*a*) S. Comby, S. A. Tuck, L. K. Truman, O. Kotova and T. Gunnlaugsson, *Inorg. Chem.*, 2012, **51**, 10158; (*b*) J. Jia, Q. C. Xu, R. C. Li, X. Tang, Y. F. He, M. Y. Zhang, Y. Zhang and G. W. Xing, *Org. Biomol. Chem.*, 2012, **10**, 6279; (*c*) X. Meng, S. Wang, Y. Li, M. Zhu and Q. Guo, *Chem. Commun.*, 2012, **48**, 4196; (*d*) T. Mukherjee, J. C. Pessoa, A. Kumar and A. R. Sarkar, *Dalton Trans.*, 2012, **41**, 5260; (*e*) S. H. Mashraqui, R. Betkar, S. Ghorpade, S. Tripathi and S. Britto, *Sens. Actuators, B*, 2012, **174**, 299; (*f*) U. C. Saha, B. Chattopadhyay, K. Dhara, S. K. Mandal, S. Sarkar, A. R. Khuda-Bukhsh, M. Mukherjee, M. Helliwell and P. Chattopadhyay, *Inorg. Chem.*, 2011, **50**, 1213.

9 (*a*) G. Mandal, M. Darragh, Y. A. Wang and C. D. Heyes, *Chem. Commun.*, 2013, **49**, 624; (*b*) G. Sivaraman, T. Anand and D. Chellappa, *Analyst*, 2012, **137**, 5881; (*c*) L. J. Liang, S. J. Zhen, X. J. Zhao and C. Z. Huang, *Analyst*, 2012, **137**, 5291; (*d*) P. G. Sutariya, N. R. Modi, A. Pandya, B. K. Joshi, K. V. Joshi and S. K. Menon, *Analyst*, 2012, **137**, 5491; (*e*) Y. W. Choi, G. J. Park, Y. J. Na, H. Y. Jo, S. A. Lee, G. R. You and C. Kim, *Sens. Actuators, B*, 2014, **194**, 343; (*f*) E. J. Song, H. Kim, I. H. Hwang, K. B. Kim, A. R. Kim, I. Noh and C. Kim, *Sens. Actuators, B*, 2014, **195**, 36; (*g*) G. J. Park, H. Kim, J. J. Lee, Y. S. Kim, S. Y. Lee, S. Lee, I. Noh and C. Kim, *Sens. Actuators, B*, 2015, **215**, 568; (*h*) J. J. Lee, S. A. Lee, H. Kim, L. T. Nguyen, I. Noh and C. Kim, *RSC Adv.*, 2015, **5**, 41905; (*i*) A. K. Bhanja, C. Patra, S. Mondal, D. Ojha, D. Chattopadhyay and C. Sinha, *RSC Adv.*, 2015, **5**, 48997; (*j*) S. Dey, A. Roy, G. P. Maiti, S. K. Mandal, P. Banerjee and P. Roy, *New J. Chem.*, 2016, **40**, 1365; (*k*) H. Y. Lin, T. Y. Chen, C. K. Liu and A. T. Wu, *Luminescence*, 2016, **31**, 236.

10 For HPO_4^{2-} sensing, see: (*a*) M. S. Han and D. H. Kim, *Angew. Chem., Int. Ed.*, 2002, **41**, 3963; for $H_2PO_4^-$ sensing, see: ref. 10*b* and *c* (*b*) S. Sen, M. Mukherjee, K. Chakrabarty, I. Hauli, S. K. Mukhopadhyay and P. Chattopadhyay, *Org. Biomol. Chem.*, 2013, **11**, 1537; (*c*) D. Zhang, J. R. Cochrane, A. Martinez and G. Gao, *RSC Adv.*, 2014, **4**, 29735; for PPi sensing, see: ref. 10*d* (*d*) S. K. Kim, D. H. Lee, J. I. Hong and J. Yoon, *Acc. Chem. Res.*, 2009, **42**, 23; for ATP sensing, see: ref. 10*e* (*e*) A. Ojida, H. Nonaka, Y. Miyahara, S. I. Tamaru, K. Sada and I. Hamachi, *Angew. Chem., Int. Ed.*, 2006, **118**, 5644; for CTP_3 sensing, see: ref. 10*f* (*f*) K. Nikura and E. V. Anslyn, *J. Am. Chem. Soc.*, 1998, **120**, 8533; for IP_3 sensing, see: ref. 10*g* (*g*) D. J. Oh and K. H. Ahn, *Org. Lett.*, 2008, **10**, 3539; for phosphoprotein sensing, see: ref. 10*h* and *i* (*h*) S. Aoki, M. Zulkefeli, M. Shiro, M. Kohsako, K. Takeda and E. Kimura, *J. Am. Chem. Soc.*, 2005, **127**, 9129; (*i*) T. Anai, E. Nakata, Y. Koshi, A. Ojida and I. Hamachi, *J. Am. Chem. Soc.*, 2007, **129**, 6232; PPi polymer sensing, see: ref. 10*j* (*j*) D. Aldakov and P. Anzenbacher Jr, *J. Am. Chem. Soc.*, 2004, **126**, 4752; for recent articles on PPi and ATP sensing, see: ref. 10*k* and *l* (*k*) X. Huang, Z. Guo, W. Zhu, Y. Xie and H. Tian, *Chem. Commun.*, 2008, 5143; (*l*) A. Ojida, I. Takashima, T. Kohira, H. Nonaka and I. Hamachi, *J. Am. Chem. Soc.*, 2008, **130**, 12095.

11 (*a*) C. P. Mathews and K. E. van Holde, *Biochemistry*, Benjamin/Cummings Publishing Company, Inc., Redwood City, CA, 1990; (*b*) P. Nyren, *Anal. Biochem.*, 1987, **167**, 235; (*c*) T. Tabary and L. Ju, *J. Immunol. Methods*, 1992, **156**, 55.

12 (*a*) X. l. Ni, X. Zeng, C. Redshaw and T. Yamato, *J. Org. Chem.*, 2011, **76**, 5696; (*b*) L. M. Mesquita, V. André, C. V. Esteves, T. Palmeira, M. N. Berberan-Santos, P. Mateus and R. Delgado, *Inorg. Chem.*, 2016, **55**, 2212; (*c*) I. Ravikumar and P. Ghosh, *Inorg. Chem.*, 2011, **50**, 4229; (*d*) S. Khatua, S. H. Choi, J. Lee, K. Kim, Y. Do and D. G. Churchill, *Inorg. Chem.*, 2009, **48**, 2993.

13 (*a*) Z. Guo, S. Park, J. Yoon and I. Shin, *Chem. Soc. Rev.*, 2014, **43**, 16; (*b*) S. Pal, S. Lohar, M. Mukherjee, P. Chattopadhyay and K. Dhara, *Chem. Commun.*, 2016, **52**, 13706.

14 (*a*) X. Lou, D. Ou, Q. Li and Z. Li, *Chem. Commun.*, 2012, **48**, 8462; (*b*) B. Sen, M. Mukherjee, S. Pal, K. Dhara, S. K. Mandal, A. R. Khuda-Bukhsh and P. Chattopadhyay, *RSC Adv.*, 2014, **4**, 14919; (*c*) D. Sarkar, A. K. Pramanik and T. K. Mondal, *RSC Adv.*, 2014, **4**, 25341; (*d*) X. Lou, H. Mu, R. Gong, E. Fu, J. Qin and Z. Li, *Analyst*, 2011, **136**, 684; (*e*) B. Sen, M. Mukherjee, S. Banerjee, S. Pal and P. Chattopadhyay, *Dalton Trans.*, 2015, **44**, 8708; (*f*) V. Bhalla, V. Vij, M. Kumar, P. R. Sharma and T. Kaur, *Org. Lett.*, 2012, **14**, 1012.

15 (*a*) L. He, C. Liu and J. H. Xin, *Sens. Actuators, B*, 2015, **213**, 181; (*b*) E. Hao, T. Meng, M. Zhang, W. Pang, Y. Zhou and L. Jiao, *J. Phys. Chem. A*, 2011, **115**, 8234.

16 W. Kabsch, *Acta Crystallogr., Sect. D: Biol. Crystallogr.*, 2010, **66**, 125.

17 M. C. Burla, R. Caliandro, B. Carrozzini, G. L. Cascarano, C. Cuocci, C. Giacovazzo, M. Mallamo, A. Mazzone and G. J. Polidori, *Appl. Crystallogr.*, 2015, **48**, 306.

18 G. M. Sheldrick, *Acta Crystallogr., Sect. A: Found. Crystallogr.*, 2008, **64**, 112.

19 D. M. Watkin, L. Pearce and C. K. Prout, *Cameron – A Molecular Graphics Package*, Chemical Crystallography Laboratory, University of Oxford, 1993.

20 W. H. Melhuish, *J. Phys. Chem.*, 1961, **65**, 229.

21 (*a*) S. Pal, M. Mukherjee, B. Sen, S. Lohar and P. Chattopadhyay, *RSC Adv.*, 2014, **4**, 21608; (*b*) S. Lohar, S. Pal, B. Sen, M. Mukherjee, S. Banerjee and P. Chattopadhyay, *Anal. Chem.*, 2014, **86**, 11357.

22 N. J. Turro, *Modern Molecular Photochemistry*, Benjamin/Cummings Publishing Co., Inc., Menlo Park, CA, 1978.

